

Transport Effects Induced by Resistive Ballooning Modes and Comparison with High- β_p ISX-B Tokamak Confinement

B. A. Carreras, P. H. Diamond, M. Murakami, J. L. Dunlap, J. D. Bell,
H. R. Hicks, J. A. Holmes, E. A. Lazarus, V. K. Paré,
P. Similon, C. E. Thomas, and R. M. Wieland

Oak Ridge National Laboratory, Oak Ridge, Tennessee 37830, and Institute for Fusion Studies, University of Texas, Austin, Texas 78712, and Computer Sciences, Nuclear Division, Union Carbide Corporation, Oak Ridge National Laboratory, Oak Ridge, Tennessee 37830

(Received 2 July 1982)

The transport effects induced by resistive ballooning modes are estimated from a theory, and are found to be mainly thermal electron conduction losses. An expression for electron thermal diffusivity χ_e is derived. The theoretical predictions agree well with experimental values of χ_e obtained from power balance for the ISX-B plasmas at high poloidal beta.

PACS numbers: 52.25.Fi, 52.30.+r, 52.55.Gb

A deterioration in confinement is observed in ISX-B tokamak experiments^{1,2} with high neutral injection power at high poloidal plasma beta (β_p). From a theoretical point of view, resistive pressure-driven ballooning modes are a possible cause of this deterioration, linked to high- β_p plasmas. There have been several linear studies³⁻⁵ of these instabilities in the past. Recently, numerical and analytical work has been done⁶ to understand the linear and nonlinear properties of resistive ballooning modes in the framework of the incompressible resistive magnetohydrodynamic (MHD) equations. Below and near the critical β for ideal instabilities ($\beta_p \geq 1$), the fastest growing mode, with a given toroidal mode number n , has a growth rate

$$\gamma_n \cong (n^2/S)^{1/3} [\beta_0 q^2 / (\epsilon \rho L_p)]^{2/3} \tau_{hp}^{-1},$$

where S is the ratio of resistive time τ_R to poloidal Alfvén time τ_{hp} , $\beta_0 = 2p(0)\mu_0/B_T^2$, p is the pressure, q is the safety factor, B_T is the toroidal magnetic field, ϵ is the inverse aspect ratio, $L_p = [(-dp/d\rho)/p(0)]^{-1}$, and ρ (with $0 \leq \rho \leq 1$) is a flux surface label. These modes are extended greatly along magnetic field lines, with a characteristic width given by

$$W_n = [q^4 \hat{S}^2 n^2 \gamma_n \tau_{hp}^{-1} / (\rho^2 S)]^{-1/4},$$

where $\hat{S} = [\rho(dq/d\rho)/q]$ and a is the minor radius. Their linear properties are similar to resistive interchanges.⁷

With use of the nonlinear resistive MHD equation in the ballooning representation, a calculation of the renormalized response has been performed.⁶ This calculation shows that the dominant nonlinear effect is due to the pressure-convective nonlinearity, which reduces the turbulent

pressure response \tilde{p} to $\tilde{\psi}$, the electrostatic perturbation. This causes a reduction of the interchange destabilizing term, without changing the basic structure of the eigenfunction. A physical interpretation is that the resistive ballooning modes saturate when the pressure fluctuation mixes $dp/d\rho$ over the radial extent Δ of each poloidal subharmonic; thus, $\tilde{p} \approx \Delta dp/d\rho$. Since the pressure is mainly convected, $\tilde{p} \approx inq\tilde{\psi}(dp/d\rho)/\rho\gamma_n$. Therefore, the kinetic energy of these modes at saturation is $E_R = \langle |(nq/\rho)\tilde{\psi}|^2 \rangle \approx \Delta^2 \times (\gamma_n \tau_{hp}^{-1})^2$. Details on the stability theory of these modes will be given elsewhere. In this Letter we limit ourselves to the consideration of the induced transport effects and consequences for confinement in ISX-B. We consider two main effects of the saturated modes, the diffusion induced by the convective nonlinearity and the anomalous electron conduction induced by the magnetic field-line stochasticization.

The radial diffusion induced by the convective term is given by

$$D \approx \langle |(n'q/\rho)\tilde{\psi}_{n'}|^2 / \gamma_{n-n'} \rangle = \gamma_n \Delta^2.$$

Using the reciprocity of y (ballooning) space and position space, $\Delta \approx (nq\hat{S}W_n/\rho)^{-1}$, we can estimate the convection losses, which are $D \approx \hat{S}^{-2}(\beta_0 q^2 / \epsilon L_p) a^2 / \tau_R$. This effect is on the order of resistive diffusion and is therefore negligible.

To calculate the induced electron conduction losses, we first calculate the magnetic-field-line diffusion coefficient D_M . It is obtained from the static-field, zero-frequency electron-drift kinetic equation for toroidal geometry, by an iterative procedure of renormalized quasilinear theory. The magnetic nonlinearity and slow radial gradients have been retained. Consistent

with conditions of the strongly turbulent regime, a renormalized propagator has been used in calculating D_M . Thus,

$$D_M = \sum_{n'} \sum_m (n'q/\rho)^2 \hat{\psi}_{n'}^* (y + 2\pi m) L_n \hat{\psi}_{n'} (y + 2\pi m)$$

where $\hat{\psi}_{n'}(y)$ is related to the poloidal flux function ψ , through the ballooning representation. The propagator is

$$L_{n'}^{-1} = i\omega_{De}/v_{\parallel} + d_{n'} + (1/Rq)\partial/\partial y,$$

with

$$d_{n'} = \sum_{n''} \sum_{m'} (n''n'q^2/\rho^2)^2 (2\pi m')^2 \hat{S}^2 \psi_{n''}^* \times (y + 2\pi m') L_{n''+n''} \hat{\psi}_{n''} (y + 2\pi m').$$

The propagator L_n can be simplified by noting that $\omega_{De}/v_{\parallel} < d_{n'}$, $d_{n'} > (RqW_n)^{-1}$ and that the rapidly oscillating pieces of $(\partial/\partial y)^{-1} \hat{\psi}_{n'}(y + 2\pi m)$ make an insignificant contribution to D_M . Therefore, $L_{n'} \approx L_{\parallel n'} \equiv d_{n'}^{-1}$, where $L_{\parallel n'}$ is the parallel correlation length for the field-line propagator $L_{n'}$. Note that in contrast to the familiar slab-model result $L_{\parallel n'} \propto D_M^{-1/3}$, here $L_{\parallel n'} \propto D_M^{-1}$.

In order to estimate D_M , it is necessary to derive an approximate expression for the relationship of $d_{n'}$ to D_M . It follows that $d_{n'} \approx (nq/\rho)^2 \hat{S}^2 W_n^2 D_M$. Thus,

$$D_M \approx (\sum_{n'} \sum_m |\hat{\psi}_{n'}(y + 2\pi m)|^2 / \hat{S}^2 W_n^2)^{1/2}.$$

Using Ohm's law to express $\hat{\psi}_{n'}$ in terms of $\hat{\phi}_{n'}$, and keeping the ordering $\gamma_n < (nq/\rho)^2 \hat{S}^2 W_n^2 / S$ gives

$$D_M \approx (SRq)^{-1} \langle (nq\hat{S}/\rho)^4 \rangle^{-1} \gamma_n W_n^{-5},$$

where the saturated value of the kinetic energy has been used to estimate $|\hat{\phi}_{n'}|^2$.

For ISX-B, $L_{\parallel n'}$ is smaller than the electron mean free path. Hence, an approximate form for the anomalous electron thermal conductivity is $\chi_e \approx \frac{3}{2} v_{Te} D_M$. Using the explicit expressions for γ and W_n , one finally finds that

$$\chi_e^{\text{Th}} \approx \frac{3}{2} (v_{Te} a) q \frac{1}{S} \left(\frac{\beta_0}{\epsilon} \frac{q^2}{S} \frac{1}{L_p} \right)^{3/2}. \quad (1)$$

Theoretical predictions based on the present model compare favorably with the results of the ISX-B beta-scaling experiments.⁸ The points of agreement between the experiment and the theory are as follows: (1) Electron heat conduction is the dominant loss channel at the high values of β_p obtained in the experiment with high-power neutral beam injection, and (2) the theoretical predictions of the electron thermal diffusivity (χ_e^{Th}) agree well over a large range of parameter varia-

tions with the values and shape of the experimental thermal diffusivity,

$$\chi_e^{\text{exp}}(\rho) = \frac{P_{be} + P_{OH} - P_{ei} - P_{rad} - \frac{5}{2} T_e \Gamma_e A_p}{(n_e A_p / a) |\partial T_e / \partial \rho|}, \quad (2)$$

based on the power balance considerations as discussed below.

The power balance is carried out in a magnetic geometry consistent with both the MHD equilibrium theory and with the available experimental observations. This is accomplished in the data analysis code ZORNOC⁹ with use of the variational moment analysis¹⁰ which incorporates (1) the experimental pressure profile, consisting of those of electrons, thermal ions, and fast ions; (2) the plasma current profile, modeled to be consistent with the radius of the $q=1$ surface observed with the soft x-ray diagnostics¹¹; and (3) the form of the outermost magnetic surface determined from the poloidal magnetic measurements.¹² The total input power consists of a large beam-power input to electrons P_{be} (calculated from classical treatments of beam deposition and slowing down) and much smaller (by factors of 5–10) Ohmic heating power P_{OH} . The ion temperature profile T_i calculated from ion power balance (with a radially constant enhancement factor for neoclassical heat conductivity¹³ adjusted to match the measured central ion temperature) is not significantly different from the electron temperature profile $T_e(\rho)$ under typical conditions, making the electron-ion heat transfer P_{ei} a small term. The radiative loss P_{rad} is small except near the edge.¹⁴ The convection loss ($\frac{5}{2} T_e \Gamma_e A_p$, where A_p is a factor which reduces to the surface area in the low- β and high-aspect-ratio limit) due to particle flux Γ_e is evaluated from particle balance with a standard neutral model,⁸ and is a small fraction of the total input. Then, the remaining power is assigned to the electron thermal conduction loss, which is by far the largest fraction of the input power. The electron temperature and density profile needed to calculate $\chi_e^{\text{exp}}(\rho)$ are based on Thomson scattering measurements along a major radius, usually at twelve separate radial positions at 3 cm intervals. Considering the uncertainties and assumptions made in the analysis, the accuracy of determining $\chi_e(\rho)$ is estimated to be within a factor of 2, which is sufficient to assess gross trends. The accuracy of evaluating χ_e^{Th} based on local experimental parameters of

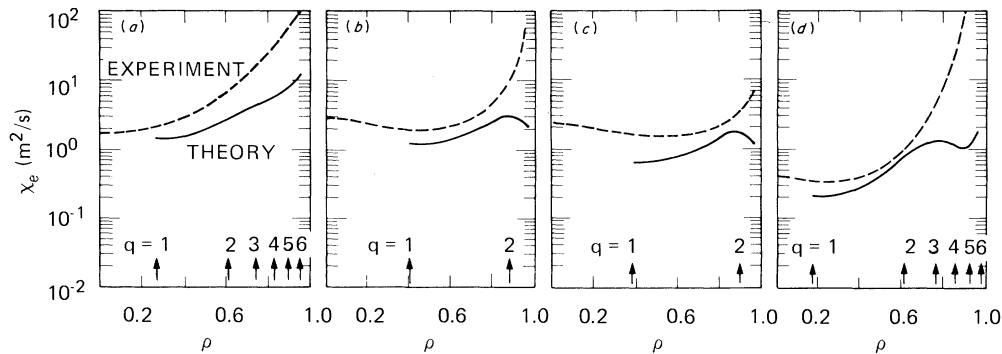


FIG. 1. Comparison of radial dependence of χ_e^{Th} and χ_e^{exp} for (a) $P_b=2$ MW, $I_p=83$ kA, $\beta_I=1.7$; (b) $P_b=2$ MW, $I_p=192$ kA, $\beta_I=1.05$; (c) $P_b=1$ MW, $I_p=184$ kA, $\beta_I=1.05$; (d) $P_b=0.6$ MW, $I_p=143$ kA, $\beta_I=0.85$.

specific ISX-B discharges is estimated to be of the same order.

Figure 1 shows the radial dependence of χ_e^{exp} and χ_e^{Th} for several typical high- β_p ISX-B discharges. The radial dependence of χ_e^{exp} is conveniently described by a three-plasma-region model: a central core region [$\rho \leq \rho(q=1)$], dominated by ($m=1, n=1$) mode and its driven modes¹¹; a confinement region outside the core where a large pressure gradient is sustained; and a plasma edge region ($\rho \approx 0.8$) dominated by atomic physics effects and/or recycling of plasma particles. As long as the central core region is not too large (which is the case for ISX-B plasmas with $q_\psi > 2.5$) and the plasma is clean, heat conduction in the confinement region determines the

confinement. Indeed, we observe that $1/\chi_e^{\text{exp}}$ in the confinement region correlates well with τ_{Ee} , the electron energy confinement time, which in turn correlates with global energy confinement time. Since the global confinement time for high-power injection plasmas in ISX-B scales differently from that in Ohmic discharges², it is not surprising that standard OH models of χ_e , all of which fit Ohmic discharges reasonably well, do not come close to χ_e^{exp} in beam-heated high- β_p discharges in either magnitude or scaling. On the other hand, the present theoretical model χ_e^{Th} fits closely the magnitude and shape of χ_e^{exp} over the large parameter ranges. Figure 2 illustrates this agreement more clearly by directly comparing χ_e^{exp} and χ_e^{Th} for scans of plasma current (at $P_b=2$ MW) and toroidal field (at $P_b=0.6$ MW).² In this figure, three χ_e values are given for the confinement region of each discharge, those at $\rho=0.50, 0.67,$ and 0.75 ; χ_e^{Th} agrees well with χ_e^{exp} over nearly two decades. Comparison of χ_e 's in a larger ISX-B data base indicates that the theoretical values are much smaller than most experimental values at low β_p ($\beta_p < 0.9$). This is expected since the ballooning

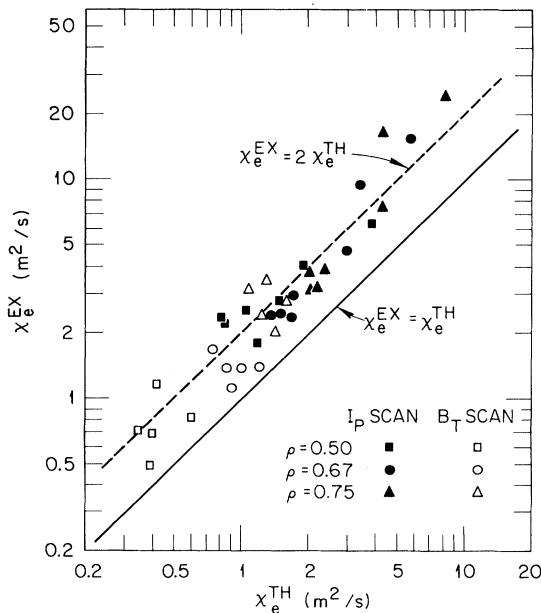


FIG. 2. Comparison of values of χ_e^{Th} and χ_e^{exp} .

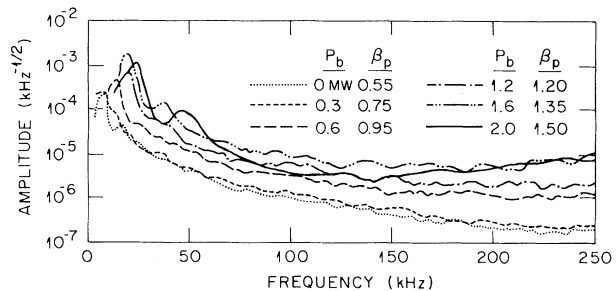


FIG. 3. Amplitude spectra of \tilde{B}_b/B_p of discharges differing in neutral-beam power.

modes are reduced at low β_p , and competing processes could easily dominate confinement. For relevant mode numbers n , the simple collisional model is applicable since γ/ω_{*e} is large. In the I_p scan, at $\rho=0.67$, the value of ω_{*e} ranges from $5 \times 10^3 n \text{ sec}^{-1}$ to $7 \times 10^3 n \text{ sec}^{-1}$ while $\gamma = 5 \times 10^4 n^{2/3} \text{ sec}^{-1}$ to $\gamma = 2.7 \times 10^4 n^{2/3} \text{ sec}^{-1}$.

Studies of the fluctuations in magnetic field near the edge of the plasma are being conducted, with Mirnov coil diagnostics, in an effort to confirm the presence of these theoretically predicted modes. The \tilde{B}_p spectra (Fig. 3) extend far beyond the range, typically 5 to 25 kHz, of the ($m=1$, $n=1$) mode.¹¹ The high-frequency tail is present independently of the ($m=1$, $n=1$).⁶ Its amplitude level increases with neutral-beam heating, and the increases develop after beam turnon in a fashion similar to the development of β_p . Details of the spectra are complex, and as yet there are no specific features that can clearly be correlated with plasma confinement. These studies continue, and similar studies are being undertaken with collimated soft x-ray diagnostics.

We acknowledge with appreciation the support of our many colleagues in the ISX-B group and in the engineering staff. We also wish to thank H. C. Howe and M. N. Rosenbluth for many useful discussions. This research was sponsored by the Office of Fusion Energy, U. S. Department of Energy, under Contracts No. W-7405-eng-26 and No. DE-FG05-80ET-53088.

¹D. W. Swain *et al.*, Nucl. Fusion **21**, 1409 (1981).

²H. G. Neilson *et al.*, to be published.

³H. P. Furth *et al.*, in *Proceedings of the Second International Conference on Plasma Physics and Controlled Nuclear Fusion Research, Culham, England, 1965* (International Atomic Energy Agency, Vienna, Austria, 1966), Vol. 1, p. 103.

⁴M. S. Chance *et al.*, in *Proceedings of the Seventh International Conference on Plasma Physics and Controlled Nuclear Fusion Research, Innsbruck, Austria, 1978* (International Atomic Energy Agency, Vienna, Austria, 1979), Vol. 1, p. 677; G. Bateman and D. B. Nelson, Phys. Rev. Lett. **41**, 1804 (1978).

⁵H. R. Strauss, Phys. Fluids **24**, 2004 (1981).

⁶B. A. Carreras *et al.*, in *Proceedings of the Ninth International Conference on Plasma Physics and Controlled Nuclear Fusion Research, Baltimore, Maryland, September 1982* (to be published), International Atomic Energy Agency Report No. CN-41/P-4.

⁷H. P. Furth, J. Killeen, and M. N. Rosenbluth, Phys. Fluids **6**, 459 (1963); B. Coppi, J. M. Green, and J. L. Johnson, Nucl. Fusion **6**, 101 (1966).

⁸M. Murakami *et al.*, in *Proceedings of the Ninth International Conference on Plasma Physics and Controlled Nuclear Fusion Research, Baltimore, Maryland, September 1982* (to be published), International Atomic Energy Agency Report No. CN-41/A-4.

⁹R. M. Wieland *et al.*, to be published.

¹⁰L. L. Lao *et al.*, Phys. Fluids **24**, 1431 (1981).

¹¹J. L. Dunlap *et al.*, Phys. Rev. Lett. **48**, 538 (1982).

¹²D. W. Swain and G. H. Neilson, Nucl. Fusion **22**, 1015 (1982).

¹³F. L. Hinton and R. D. Hazeltine, Rev. Mod. Phys. **48**, 239 (1976).

¹⁴C. E. Bush *et al.*, to be published.